

# Design of a Compliance Assisted Quadrupedal Amphibious Robot

Andrew R. Vogel<sup>1</sup>, Krishnanand N. Kaipa<sup>2</sup>, Gregory M. Krummel<sup>3</sup>,  
 Hugh A. Bruck<sup>4</sup>, and Satyandra K. Gupta<sup>5</sup>

**Abstract**—This paper describes RoboTerp, a quadrupedal amphibious robot that achieves locomotion on land and in water with the same legs by switching gaits to match the terrain. The central idea hinges on a passive compliant mechanism attached to the lower leg that enables it to behave like a valve during movement in water. The direction of this valve-like mechanism is aligned such that rhythmic oscillations of the legs generate a net thrust that propels the robot forward in water. By design, this oscillatory leg movement achieves splash-free swimming, and thereby overcomes the shortcomings of most previous wheel-leg based designs, in which rotational movement causes water splashing that leads to significant turbulence in the robot surroundings. We examined different materials and morphological parameters to select the best flap configuration. A modular design allowed rapid iterations of these experiments. We confirmed the performance of the best few configurations found during the experiments through fluid simulations. Finally, we report successful demonstrations of RoboTerp walking on asphalt land, swimming in a pool, and transitioning between uneven rock surface and water in an outdoor creek.

## I. INTRODUCTION

Mobile robots used in outdoor applications—search, rescue, and monitoring—are traditionally designed to handle complexities of a single terrain (either land or water). As the design requirements significantly differ from one terrain to another, terrestrial robots fail to operate in water; likewise, purely aquatic robots are unable to locomote on land. Although aerial robots can hover over land and water, considerable tree cover typically present in semi-aquatic regions like swamps and creeks limits their operational effectiveness to a great extent. These issues and a growing demand for amphibious robots have motivated researchers to find solutions to amphibious robotic locomotion recently.

Nature provides a primary source of inspiration: amphibious animals and insects have evolved particular morphological, biomechanical, and control structures that enable them to navigate effortlessly on both land and water. Accordingly, there have been some research attempts over the past decade to build robots that replicate mechanisms of amphibious

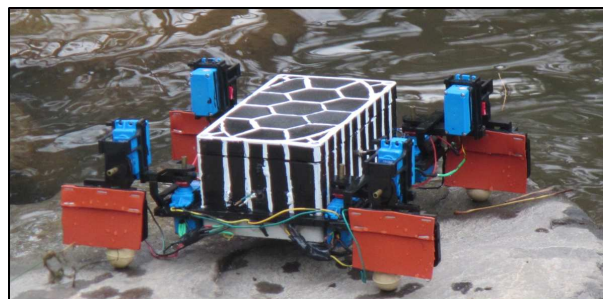


Fig. 1. RoboTerp navigating in an outdoor creek.

locomotion found in nature [1], [2], [3], [4], [5], [6]. Further, purely engineering based solutions have been pursued to some extent [7], [8], [9], [10].

However, the design of amphibious robots still presents several important open ended challenges: (1) Separate mechanisms (e.g., wheels/legs for land and fins/paddles for water) can be combined to achieve amphibious capability in robots. However, without a careful design, this method can become cumbersome and inefficient due to an increase in the number of actuators. This raises the question of whether actuated and passive members can be integrated into a single mechanism to produce amphibious propulsion. (2) Waterproofing is a principal design requirement for a robot operating in aquatic terrains and must be addressed head on. (3) A detailed study of how different configurations—body plans, materials, and gaits—impact locomotion efficiency (by using fluid simulations and experiments involving thrust measurements) must be carried out in order to select the best configuration for the robot. This calls for a modular design that allows rapid iterations of all variants of the physical platform.

In this paper, we present the design of RoboTerp, a quadrupedal amphibious robot that achieves locomotion on land and in water with the same legs by switching gaits to match the terrain. In most earlier amphibious robots based on either compliant legs or wheel-leg mechanisms, the legs rotate in order to generate propulsion in water. During each rotation cycle, the legs lift off from the water surface into the air and splash back into the water. This causes significant disruptive turbulence in the surroundings of the robot. Therefore, we have taken a different approach. Our leg mechanism is designed in such a way that rather than using a rotational motion, it uses an oscillatory motion in order to generate forward thrust in water. This thereby allows it to perform splash-free swimming. In particular, the central

<sup>1</sup>Andrew Vogel is a graduate student at the Department of Mechanical Engineering, University of Maryland, College Park, MD, USA avogel2@umd.edu

<sup>2</sup>Krishnanand Kaipa is a Research Assistant Professor at the Department of Mechanical Engineering, University of Maryland, College Park, MD, USA kkrishna@umd.edu

<sup>3</sup>Gregory Krummel is an undergraduate student at the Department of Mechanical Engineering, University of Maryland, College Park, MD, USA g.m.krummel@gmail.com

<sup>4</sup>Hugh Bruck is a Professor at the Department of Mechanical Engineering, University of Maryland, College Park, MD, USA bruck@umd.edu

<sup>5</sup>Satyandra Gupta is a Professor at the Department of Mechanical Engineering and Institute for Systems Research, University of Maryland, College Park, MD, USA skgupta@umd.edu

idea hinges on a passive compliant appendage attached to the lower leg structure that enables it to behave like a valve in the presence of water. The direction of this valve-like mechanism is aligned such that rhythmic oscillations of all the four legs generate a net forward thrust that enables the robot to transition to, and perform, surface swimming in semi-aquatic terrains.

We examined different combinations of materials (flap thickness and hardness) and morphological factors (orientations of flap and knee axes) in order to select the best configuration of the compliant flap mechanism. We confirmed the performance of the best few configurations found during the experiments through fluid simulations. Successful physical demonstrations involving walking on asphalt land, swimming in a pool, and transitioning gaits between uneven rock surface and water in an outdoor creek validate the robot's effectiveness in real terrains.

## II. RELATED WORK

ACM-R5 [2], a snake-like robot achieved locomotion both in water and on land by using undulation and wheels on independent segments. Amphibot [3], [11], [12], another snake-like robot, similarly used undulation in conjunction with passive wheels in order to crawl on land and swim in water. The passive wheels of Amphibot were replaced by four simple legs to give rise to a Salamander-like amphibious robot [13] that was capable of terrestrial motion and surface transition. Another AmphiRobot [4] used composite propulsion (comprising body undulations, a wheel-propeller-fin mechanism in the front, and a caudal fin in the rear) to achieve a fish-like swimming pattern.

RHex [14], a highly rugged hexapod, used compliant legs with only six actuated degrees of freedom. Several variants of this six-legged robot were built to produce amphibious propulsion: In the first version of AQUA [5], [15], the rigid legs of RHex had to be manually replaced by paddles for the sake of swimming. In the second version, the same compliant flippers were used for propulsion in both land and water. However, this had a significant negative impact on its ability to walk.

AmphiHex-I [6], inspired by AQUA, attempted to rectify these shortcomings by using transformable leg-flippers that could actively switch between curved shaped legs (for propulsion on land) and straight shaped paddles (for propulsion in water). ASGUARD [9] eschewed RHex's six legs in favor of four wheel-like spokes, which granted it significant mobility on land and some motion while floating on water, albeit at the cost of significant water disturbance. Whogs [7], [8] used wheel-legs to walk on both land and the ocean floor, and to swim over obstacles. eQuad [10] used a combination of eccentric paddles and wheels to achieve locomotion in both terrestrial and aquatic terrains.

In all the above examples based on either compliant legs or wheel-leg mechanisms, the legs rotate in order to generate propulsion in water. As mentioned earlier, this causes a disruptive turbulence in the surroundings of the robot. However, our leg mechanism uses an oscillatory motion in order to

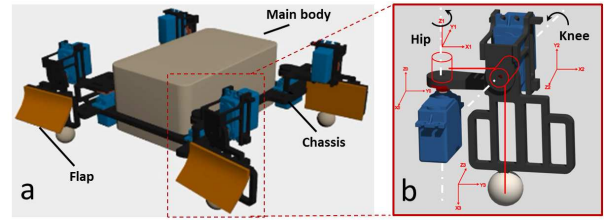


Fig. 2. (a) 3D model of RoboTep in an outside-front and outside-back configuration. (b) Close-up view of the leg design (The flap is removed to reveal the interior structure of the leg).

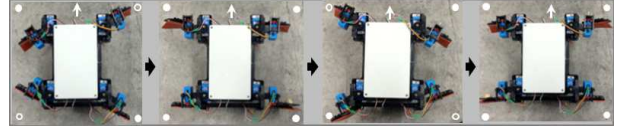


Fig. 3. Trot gait used by RoboTep to walk on land. For each foot, a white circle next to it indicates that the foot is in air and a white dot indicates that it is on ground.

generate forward thrust in water. This thereby allows it to perform splash-free swimming. A simple, efficient method of changing between terrestrial to aquatic locomotion is used so that the robot is positioned effectively to resume movement post-transition.

## III. PHYSICAL ROBOT

A snapshot of RoboTep in a creek is shown in Fig. 1. A 3D model (Fig. 2) is used to illustrate its mechanical construction: the robot structure consists of (1) a main body that serves as a waterproof casing for the electronics, (2) four legs—each with two actuated joints and a passive compliant flap—designed for amphibious locomotion, and (3) a rectangular chassis that houses the main body and the four legs. High-torque waterproofed servo motors with ingress protection from submersion in water are employed; all remaining electronics are protected within a waterproofed casing. Transition from land to water and vice versa is sensed by exposed electrical contacts that close (open) a circuit in the presence (absence) of water, typically found in creeks, ponds, and lakes. Additionally, three bump-activated switches were added on the front of the robot to facilitate transition from water to land. These sensors and all eight servomotors are interfaced to an Arduino Mega 2560 microcontroller. The robot is powered by a 6-volt, 2000 mAh nickel metal hydride battery (for servomotors) and a 9-volt alkaline battery (for Arduino). The robot weighs 1.72 kg. The footprint of the robot is 29.2 cm  $\times$  20.0 cm. The robot can operate for roughly 20 minutes on a single battery charge.

### A. Leg Design for Amphibious Locomotion

The main idea behind the design of the leg mechanism lies in the fact that the same legs that achieve locomotion on land using one gait, also provide propulsion in water by switching to a different gait. First, we describe the part of the leg mechanism that achieves walking.

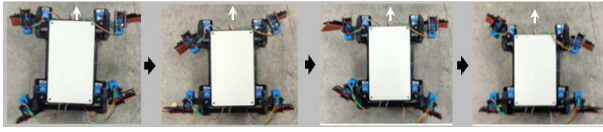


Fig. 4. Walking gait used by RoboTerp to move in shallow waters.

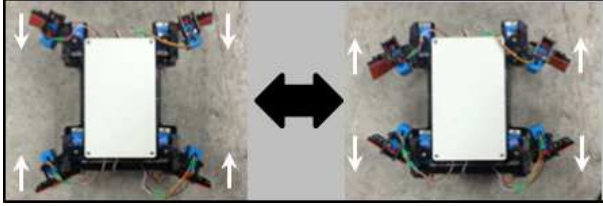


Fig. 5. Swimming gait used by RoboTerp to move in deep waters.

*Design of rigid legs for walking:* Each leg is based on a simple two DOF design that is well examined in the literature. The leg configuration is shown in Fig. 2(b). Each leg consists of two actuated joints: (a) *Hip*: The hip joint is located close to the body and allows the robot to sweep the leg from backward to forward and vice versa. (b) *Knee*: The knee joint is suspended at the end of the upper leg and allows the robot to lift the lower leg off the ground during recovery phase. As shown in the figure, the lower leg is both unusually shaped and longer than the upper leg; although these morphological properties do not affect walking, they facilitate the swimming mechanism, which is explained next.

*Design of compliant mechanism for swimming:* The compliant flap attached to the lower leg (Fig. 2(a)) uses a valve-like mechanism to generate forward thrust. For this purpose, the hip joint is actuated, while the knee joint motion is frozen. Now, as the leg performs a forward stroke (this relates to the sweep movement in the horizontal plane from front to back of the robot), the interaction with water causes the flap to snap to the flanged leg frame, thereby resisting any water flow through the interior of the lower leg. The resulting reaction force propels the body forward. However, as the leg performs a recovery stroke (sweep movement in the horizontal plane from back to front), the flap deforms away from the leg, thereby allowing water flow through the interior of the lower leg. The effect of this is to avoid drag during the recovery stroke. Therefore, each swimming gait cycle consists of a forward stroke and a backward stroke with a net forward thrust, maintained through repeated oscillation.

### B. Design of Gaits

Three primary gaits of trotting, walking, and swimming are created for locomotion on land, in shallow water that is not deep enough for floatation, and in deep water. Handling these particular situations are essential to operating in semi-aquatic terrains. The trotting and walking gaits each have a 150 ms delay between two steps, and the swimming gait has a 250 ms delay between two steps. Two transition gaits are also synthesized for the purpose of aiding the change



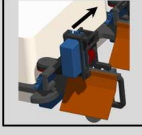

Parameter	Values			
Flap thickness (mm)	0.79	1.59	2.38	3.175
Flap hardness (A durometer)	10	40	60	
Flap axis	 Horizontal		 Vertical	
Knee axis	 Inside		 Outside	

Fig. 6. Parameters used to evaluate different morphological configurations.

between walking/trotting and swimming.

As can be seen in Fig 3, trotting is a four-step gait which has either two or four feet on the ground during any given step. Diagonal leg pairs act in tandem as the feet take up a triangular motion pattern. In less steady conditions, such as walking in shallow water, stability is more of a priority than speed. The walking gait (Fig. 4) is similar to the trotting gait in terms of the triangular foot movement, but different in that there is no symmetry to it: each leg is at a different place in the four-step triangular pattern at any given time. This allows the robot to have three feet on the walking surface at any time, which greatly increases stability in an unsteady terrain. The swimming gait involves sweeping the legs back and forth and using compliance in order to create a net forward thrust. Specifically, as shown in Fig. 5, the knee joints are frozen, while the hip joints oscillate. The front legs and back legs operate symmetrically to avoid incidental movement from side to side while swimming.

The purpose of land-to-water transition gait is to establish an initial four-legged push to create initial forward velocity and to clear away from land. All four legs are placed forward and then propelled backward before the back legs are positioned in the configuration used for swimming. During water-to-land transition, the robot must be able to pull itself on whatever surface is detected on the shore. For this purpose, each front leg is lifted up and moved forward before both legs are retracted to propel the robot out of the water.

## IV. ANALYSIS OF COMPLIANT MECHANISM

### A. Design Variants

Different combinations of parameters like flap thickness, flap hardness, flap axis, and knee axis were examined in order to select the best configuration of the compliant flap



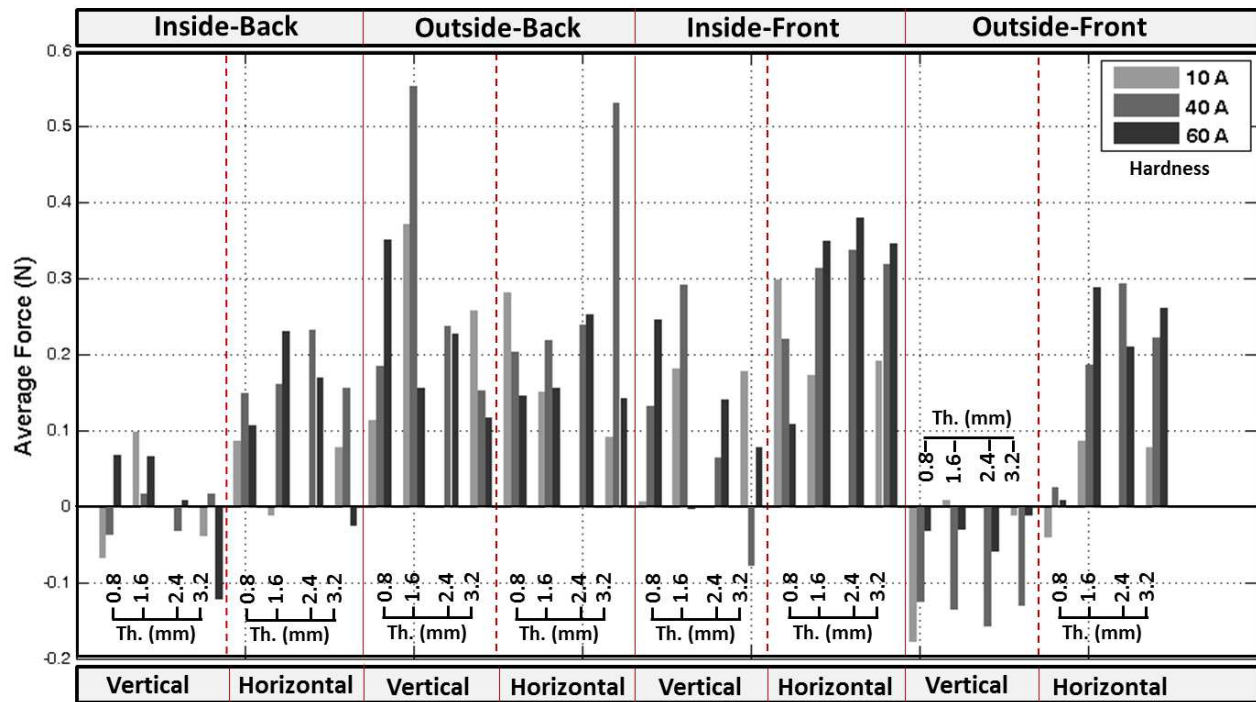


Fig. 7. Forward propulsion thrust results for various combinations of design parameters.

mechanism. These design iterations were carried out experimentally; the performance of the best few configurations found during the experiments were confirmed through fluid simulations.

The four parameters and their values are shown in Fig. 6. The flaps are made of silicone rubber. With the exception of 2.38 mm / 10A durometer rubber (absent due to supplier availability) all other combinations shown in the figure were considered. Two lower leg designs that support a horizontal flap axis and a vertical flap axis, respectively, were considered. Two orientations of the knee axis were considered. In particular, an inside configuration points the servomotor spline axis of the knee joint toward the center of the robot, while an outside configuration points servomotor spline axis away from the robot. This is important with respect to the direction of compliance relative to the knee motor housing: inside-front and outside-back configurations have the compliant direction pointed away from the motor housing, while the outside-front and inside-back configurations let the flaps bend toward the motor housing during recovery. Whereas the final robot used an outside-front and outside-back configuration (as shown in Fig. 2(a)) to achieve simplicity in balancing for terrestrial movement, experimental evaluations of inside configurations were deemed useful for the sake of identifying possible trends in the results.

#### B. Experimental Setup

The thrust produced by the legs was measured by placing the robot in a tub of water with one end connected by a 5 lb, one DOF force sensor to the edge of the tub. To

compensate as much as possible for vertical bobbing, the force sensor was attached to the tub wall at the equilibrium point for floating. While horizontal motion was not explicitly restrained, the symmetrical nature of the swimming motion limited significant horizontal drifting during testing. For the purpose of determining relative contribution of front and back leg pairs, each pair was tested separately, by freezing the motion of the other pair of legs.

Each test was ten seconds long, with the force sensor taking measurements at a rate of 1kHz. The measurements were recorded using LabVIEW. In the interest of avoiding any initial transients and measuring only the steady-state oscillations, data during the first second (correspondingly, the first thousand data points) were discarded. The remaining 9000 data points were used in the force calculations. A baseline test was used to determine the conversion factor, which was then used to convert the voltage measurements from the sensor into force measurements.

#### C. Experimental Results

The thrust results are shown in Fig. 7. Performances of all tested configurations are presented in the same graph for an easier comparison between design variants. In particular, the results are divided into four sets according to inside-back, outside-back, inside-front, and outside-front configurations, respectively. Further, in each set, the results for horizontal flap-axis and vertical flap-axis are presented next to each other in two subsets. Each subset consists of four groups (corresponding to four thickness values of the flap), with three bars in each group (corresponding to three hardness

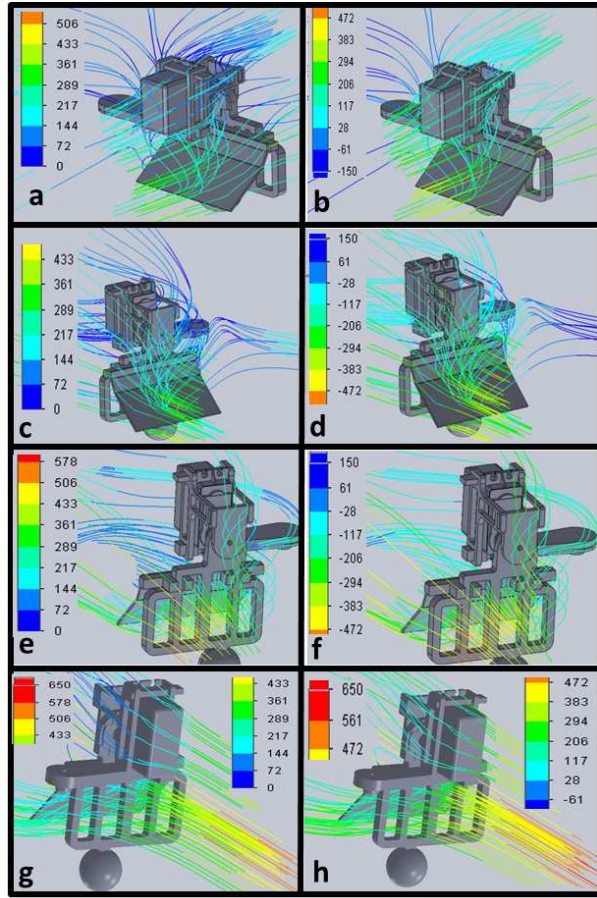


Fig. 8. (a) Anti-spline thrust absolute velocity profile varies from 0 to 506 mm/s. (b) Anti-spline thrust directional velocity profile varies from -150 to 472 mm/s. (c) Pro-spline thrust absolute velocity profile varies from 0 to 433 mm/s. (d) Pro-spline thrust directional velocity profile varies from -470 to 150 mm/s. (e) Anti-spline recovery absolute velocity profile varies from 0 to 578 mm/s. (f) Anti-spline recovery directional velocity profile varies from -472 to 150 mm/s. (g) Pro-spline recovery absolute velocity profile varies from 0 to 650 mm/s. (h) Pro-spline recovery directional velocity profile varies from -61 to 650 mm/s.

values of the flap). Note that there are only two bars for each 2.4 mm combination as the 2.4 mm/10A flap was not tested due to reasons mentioned in Section IV A.

The primary conclusion from this set of results was that the performance of flaps with horizontal-axis was better than that of flaps with vertical-axis in most cases. This is true in general for the three configurations of inside-back, inside-front, and outside-front. Note that in the case of outside-back configuration, the performances of horizontal and vertical configurations are comparable to each other. Further, inside-front and outside-back legs performed better than outside-front and inside-back legs. Among the thickness and hardness combinations, the 1.59 mm /40 A durometer and 2.38 mm / 40 A durometer flaps performed the best. The thrust contributions of the front and back legs were found to be approximately equal. The negative thrust for the vertical outside-front configuration is likely due to an extremely low thrust combined with reflection-based errors.

#### D. Simulation Setup

To verify these results, the two rubber types that performed best were selected for further exploration via fluid simulation. This was performed using SolidWorks 2012's flow simulation package. For this purpose, a static leg model constructed in Pro Engineer with bending flaps represented by a series of two static plates placed at the same angle was considered with the water flow in a manner representative of the water flowing around the leg as it propels the robot in still water. The oscillation velocity  $V_O$  was calculated by multiplying the observed oscillation frequency  $f$  ( $= 2.34$  Hz), the  $120^\circ$  oscillation cycle converted to 2.09 radians, and the radius  $r$  at any point. The forward velocity  $V_F$  was calculated by observation of previous models. Combined, they created the total thrust velocity  $V_T$  and total recovery velocity  $V_R$ ; these equations were used to model the flow in the simulations. The magnitude of velocity operates under the convention that positive velocity is in the direction of robot motion, while a negative sign opposes the direction of motion.

$$|V_O| = 4.89 \times r \text{ mm/s} \quad (1)$$

$$V_F = 71.882 \text{ mm/s} \quad (2)$$

$$V_T = 4.89r - 71.882 \text{ mm/s} \quad (3)$$

$$V_R = -4.89r - 71.882 \text{ mm/s} \quad (4)$$

As with the experimental testing, the two rubber types were tested with each combination of flap axis, knee axis, and leg pair; outside-back and inside-front configurations were combined into a group designated as pro-spline. Likewise, outside-front and inside-back configurations were combined into an anti-spline group. Each flap surface was considered as a smooth surface at a roughness of 0 micro inches. Pressure and temperature were set to 1 atmosphere and 20.05 degrees celsius, respectively.

#### E. Simulation Results

Simulations results coincided with experimental findings. Horizontal-axis flaps outperformed vertical-axis flaps, while pro-spline configurations outperformed anti-spline configurations for both thrust and recovery. Both absolute and directional velocities were examined. The comparison of anti-spline and pro-spline can be seen in Fig. 8(a–h). It can be observed that the absolute and directional velocities of water upon the flap are greater for pro-spline configurations compared to anti-spline. This holds for both thrust and recovery and lends itself to more responsive, and thus more efficient, compliant mechanisms. The perceived reason for this difference was diffusion of incoming water by the motor housing in anti-spline configurations.

Based on the above analysis, the configuration chosen for the final prototype of RoboTerp used a leg design with a horizontal flap axis. Inside-front and outside-back legs performed better in the experiments. This was also confirmed in simulations (pro-spline configuration). However, this choice was less feasible due to the necessity of symmetrical legs for walking balance. Therefore, the final robot used outside-front and outside-back legs. Both flaps with thickness/hardness



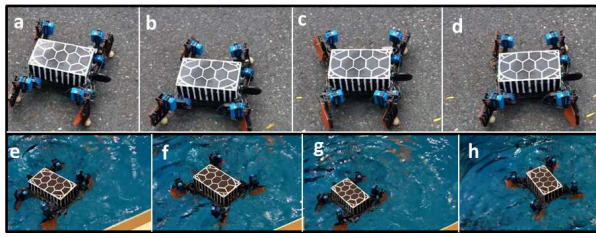


Fig. 9. (a–d) RoboTerp walking on land (asphalt surface). (e–h) RoboTerp swimming in a neutral buoyancy tank.

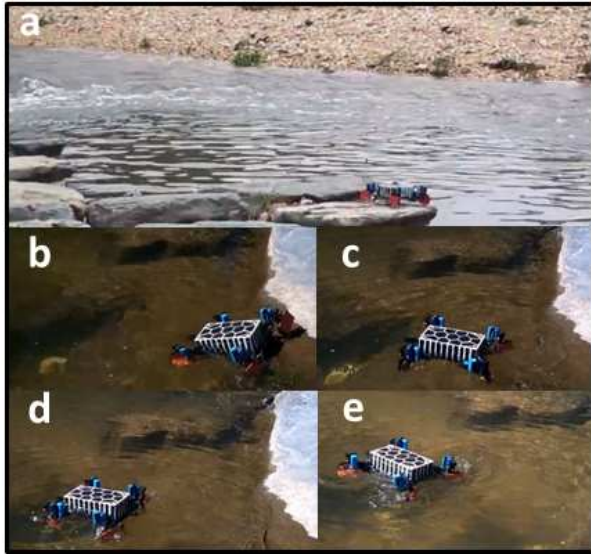


Fig. 10. (a) RoboTerp tested in an outdoor creek. (b–d) RoboTerp transitioning from land to water and swimming thereafter.

combinations of 1.59 mm /40 A durometer and 2.38 mm / 40 A durometer were selected for final testing.

## V. FIELD TESTING

RoboTerp was tested in a variety of terrains. Initially, the robot was made to walk on asphalt land. Figures 9(a–d) shows snapshots from a video footage of RoboTerp walking successfully on asphalt land. Next, the surface swimming capability of RoboTerp was tested in a neutral buoyancy tank (Fig. 9(e–h)). Finally, RoboTerp was tested for walking, swimming, and transitioning in an outdoor creek (Fig. 10(a)). Figure 10(b–f) shows snapshots from a video footage of RoboTerp walking on a rock, switching to a swimming gait as it transitions into water, and swimming thereafter.

## VI. CONCLUSIONS

We developed a low-cost amphibious robot with mainly off-the-shelf components. The robot achieved splash-free swimming by utilizing compliance assisted legs and oscillatory leg movements. This reduces energy needed for swimming. We designed and demonstrated appropriate walking and swimming gaits. We integrated sensors to trigger transition between swimming and walking and successfully

demonstrated transition between walking and swimming using sensors. Future direction of work will include (1) development of minimal energy gaits, (2) concurrent gait and flap optimization to increase forward velocity, and (3) integration of vision-based sensors.

## ACKNOWLEDGMENT

Dr. S.K. Gupta's participation in this research was supported by National Science Foundation's Independent Research and Development program.

## REFERENCES

- [1] A. J. Ijspeert, A. Crespi, D. Ryczko, and J.-M. Cabelguen, "From swimming to walking with a salamander robot driven by a spinal cord model," *Science*, vol. 315, no. 5817, pp. 1416–1420, 2007.
- [2] S. Hirose and H. Yamada, "Snake-like robots [tutorial]," *Robotics and Automation Magazine, IEEE*, vol. 16, no. 1, pp. 88–98, 2009.
- [3] A. Crespi, A. Badertscher, A. Guignard, and A. Ijspeert, "Swimming and crawling with an amphibious snake robot," in *Robotics and Automation, 2005. ICRA 2005. Proceedings of the 2005 IEEE International Conference on*, 2005, pp. 3024–3028.
- [4] R. Ding, J. Yu, Q. Yang, M. Tan, and J. Zhang, "Robust gait control in biomimetic amphibious robot using central pattern generator," in *Intelligent Robots and Systems (IROS), 2010 IEEE/RSJ International Conference on*, 2010, pp. 3067–3072.
- [5] G. Dudek, P. Giguere, C. Prahacs, S. Saunderson, J. Sattar, L. Torres-Mendez, M. Jenkin, A. German, A. Hogue, A. Ripsman, J. Zacher, E. Milios, H. Liu, P. Zhang, M. Buehler, and C. Georgiades, "Aqua: An amphibious autonomous robot," *Computer*, vol. 40, no. 1, pp. 46–53, 2007.
- [6] X. Liang, M. Xu, L. Xu, P. Liu, X. Ren, Z. Kong, J. Yang, and S. Zhang, "The amphiHex: A novel amphibious robot with transformable leg-flipper composite propulsion mechanism," in *Intelligent Robots and Systems (IROS), 2012 IEEE/RSJ International Conference on*, 2012, pp. 3667–3672.
- [7] A. Boxerbaum, P. Werk, R. Quinn, and R. Vaidyanathan, "Design of an autonomous amphibious robot for surf zone operation: part i mechanical design for multi-mode mobility," in *Advanced Intelligent Mechatronics. Proceedings, 2005 IEEE/ASME International Conference on*, 2005, pp. 1459–1464.
- [8] R. Harkins, J. Ward, R. Vaidyanathan, A. Boxerbaum, and R. Quinn, "Design of an autonomous amphibious robot for surf zone operations: part ii - hardware, control implementation and simulation," in *Advanced Intelligent Mechatronics. Proceedings, 2005 IEEE/ASME International Conference on*, 2005, pp. 1465–1470.
- [9] M. Eich, F. Grimmering, and F. Kirchner, "A versatile stair-climbing robot for search and rescue applications," in *Safety, Security and Rescue Robotics, 2008. SSR 2008. IEEE International Workshop on*, 2008, pp. 35–40.
- [10] Y. Sun and S. Ma, "Decoupled kinematic control of terrestrial locomotion for an epaddle-based reconfigurable amphibious robot," in *Robotics and Automation (ICRA), 2011 IEEE International Conference on*, 2011, pp. 1223–1228.
- [11] A. Ijspeert and A. Crespi, "Online trajectory generation in an amphibious snake robot using a lamprey-like central pattern generator model," in *Robotics and Automation, 2007 IEEE International Conference on*, 2007, pp. 262–268.
- [12] A. Crespi and A. Ijspeert, "Online optimization of swimming and crawling in an amphibious snake robot," *Robotics, IEEE Transactions on*, vol. 24, no. 1, pp. 75–87, 2008.
- [13] A. Crespi, K. Karakasiliotis, A. Guignard, and A. Ijspeert, "Salamandra robotica ii: an amphibious robot to study salamander-like swimming and walking gaits," *Robotics, IEEE Transactions on*, vol. 29, no. 2, pp. 308–320, April 2013.
- [14] E. Z. Moore, D. Campbell, F. Grimmering, and M. Buehler, "Reliable stair climbing in the simple hexapod 'rhex'," in *Robotics and Automation, 2002. Proceedings. ICRA '02. IEEE International Conference on*, vol. 3, 2002, pp. 2222–2227.
- [15] J. Sattar, P. Giguere, G. Dudek, and C. Prahacs, "A visual servoing system for an aquatic swimming robot," in *Intelligent Robots and Systems, 2005. (IROS 2005). 2005 IEEE/RSJ International Conference on*, 2005, pp. 1483–1488.